Cooperative Laser/Collision-Induced Chemical Bonds

KAI-SHUE LAM

Department of Physics, California State Polytechnic University, Pomona, California 91768

THOMAS F. GEORGE*

Departments of Chemistry and of Physics & Astronomy, State University of New York at Buffalo, Buffalo, New York 14260

Received April 28, 1986 (Revised Manuscript Received September 15, 1986)

Contents

I. Introduction

The laser has long been advocated as an invaluable tool for inducing state-specific dynamical processes in atoms and molecules and is thus the ideal agent for "controlling" chemical reactions.[1] In the early phases of laser photochemistry, it was used mainly as an excitation agent for certain atomic/molecular species, which were then brought into close proximity with other atomic/molecular species to produce chemical reactions. Later, it was realized that the laser, in addition to being an excitation agent, can also change the nuclear dynamics during an atomic/molecular encounter.[2] The latter possibility, for a while, appeared to move chemists significantly closer to the claim that laser photochemistry may fulfill the age-old dream of alchemy.

The main advantage of this second possibility is that the absorbed photons need not be in resonance with specific asymptotic energy levels of the atomic/molecular species involved in the collision process. A photon detuned from resonance can still be absorbed, the difference in energy being made up by the "distortion" of electronic energy levels during the collision. Moreover, this "distortion" may be further changed by the laser field itself in such a way as to enhance the breaking or formation of chemical bonds. Thus light absorption and collisional energy transfer need not be independent events.

The price to pay for this scenario is the high power of the laser that is usually required. For the laser field to change molecular dynamics, photons must be absorbed within time scales of the order of collision times, typically 10^{-13} s. The large transition rate then requires laser powers (proportional to the square of the radiative coupling energy) of the order of 10^9–10^{12} W/cm^2. While experiments have been performed successfully using high-ower lasers,[3-13] the very stringent power requirements have prevented them from being versatile tools. As a result, the optimism initially associated with high-power laser photochemistry has somewhat abated, and focus has recently been redirected towards making the optimal use of moderate power lasers.[14,15]

A subject of much interest regarding the use of moderate-power lasers is the formation of chemical bonds with the help of lasers. Aside from the intrinsic interest in chemical bonds themselves, bound states in the nuclear degrees of freedom are also of great importance in laser photochemistry, since these can serve as initial states from which laser photons are absorbed. The absorption can now take place from the stabilized collision complex over much longer time intervals than collision times, and consequently the power requirement for the laser becomes much less severe. Thus free–bound transitions exploiting moderate-power lasers may achieve the same goals as free–free transitions which are only possible with the help of very intense lasers. These free–bound collisions (associative or dissociative) are sometimes referred to as half-collisions, and for them the laser is again recognized as a most significant inducing agent. In the same spirit, laser-induced bound–bound transitions, such as stabilization of an excited complex by stimulated emission to a lower or ground vibrational state, has been found to be important in isotope separation.[16] This process is referred to as laser-induced preassociation. We should also mention here before going further that since our focus is on bond formation due to bound–free transitions, we are excluding the general area of chemical reactions,

0009-2665/87/0787-0155$06.50/0

Kai-Shue Lam was born in 1949 in Hong Kong. He received his B.A. degree in physics from the University of California at Berkeley in 1970 and his Ph.D. degree in physics from the Massachusetts Institute of Technology in 1976. He then spent successive years in the Chemistry Department of the University of Rochester as Postdoctoral Fellow, Research Associate, and Senior Research Associate. In 1984 he joined the faculty of the Physics Department of the California State Polytechnic University at Pomona, where he is at present Associate Professor of Physics. Dr. Lam's research interests include atomic and molecular dynamics and its interaction with laser radiation. He is a member of the American Physical Society.

Thomas F. George was born in 1947 in Philadelphia, PA. After receiving his Ph.D. degree in chemistry from Yale University in 1970, he spent successive years as a Research Associate at MIT and the University of California at Berkeley. He joined the faculty of the University of Rochester in 1972 as Assistant Professor of Chemistry and was promoted to Associate Professor in 1974 and to Professor in 1977. In 1985 he moved to the State University of New York at Buffalo as Dean of Natural Sciences and Mathematics/Professor of Chemistry and Physics. His awards and honors include: Dreyfus Teacher–Scholar, 1975–1985; Sloan Fellow, 1976–1980; Marlow Medal and Prize from the Royal Society of *Chemistry*, 1979; *New York Academy of Sciences* Fellow, 1981–; Guggenheim Fellow, 1983–1984; American Physical Society Fellow, 1984–. He has served on the advisory/editorial boards of *Chemical Physics Letters*, *The Journal of Physical Chemistry*, and *Molecular Physics*. He was Chairman of the Gordon Research Conference on Molecular Energy Transfer in 1981. He has served on the Executive Committee of the Physical Division of the American Chemical Society and is Chairman-Elect for 1986–1987. In 1986 he was named to the Board of Managers of the Buffalo Museum of Science. Dr. George's research interests include molecular energy transfer, reaction dynamics, and the interaction of laser radiation with molecular rate processes in the gas phase and at a gas-solid interface. Attention has been focused recently on the development of theoretical techniques and computer codes to describe a variety of surface processes such as: desorption, migration, chemical vapor deposition, grating growth of metal films on semiconductor substrates, charge transfer in ion–surface scattering, resonance fluorescence, surface-state excitation, and electron–hole pair formation by molecule–semiconductor collisions. There is special interest in microstructures and cluster phenomena. His research activities have led to 250 publications and 150 invited conference lectures/seminars/colloquia.

where bond formation is accompanied by bond breaking (this area has received some experimental attention[6,9,12] and a fair amount of theoretical attention by us and others, which we do not reference here).

Typically the laser is used to excite a nuclear bound state through photon absorption or to populate a bound state through stimulated emission. For the diatomic case with which we will be mainly concerned in the present article, these processes can be represented as

$$A + B + \hbar\omega \rightarrow AB^* \quad \text{absorption}$$

$$A + B^* + \hbar\omega \rightarrow AB + 2\hbar\omega \quad \text{stimulated emission}$$

In the latter case the incident photon is not absorbed, and one extra photon of the same mode is deposited into the radiation field. Interesting theoretical studies of these processes have been carried out by various investigators.[17-19] Some significant results include the following. In the absorption case, interference between the radiative preassociation and natural predissociation (due to the presence of continuum nuclear states crossing the excited-bound state) is stressed.[17] In the emission case, an associative mechanism due to the deexcitation of a Feshbach resonance to a truly bound nuclear state is proposed.[18]

On the experimental side, photoassociative laser-induced fluorescence studies have been carried out for heavy-metal eximers such as Hg_2[20] and rare-gas–halide exciplexes such as XeCl[21] and XeBr.[22] These spectroscopic studies typically involve laser excitation from a repulsive or very weakly bound van der Waals potential to a bound-excited vibronic state of high vibrational quantum number. The resulting fluorescence profiles then provide valuable information for the inner portion of the repulsive (or weakly bound) ground-state potential which may be very difficult to probe with other techniques. If the ground state is a free (continuum) state, a characteristic oscillatory profile results. This oscillatory effect has been called "Condon internal diffraction",[20] and very often can be explained in terms of the Franck–Condon principle of local (vertical) electronic transitions (nuclear configurations unchanged). In this case, the Franck–Condon overlap integral of the excited-bound-state nuclear wave function and the ground-state continuum wave function is the determining factor in the fluorescence line shape.

Another type of important photoassociative process is laser-induced associative ionization,

$$A^* + B + \hbar\omega \rightarrow AB^+ + e^-$$

Although in general the nature of the mechanisms of ionized-dimer production remains controversial, it has been suggested[23] that two of the most important ones are laser-induced associative ionization and molecular multiphoton ionization of neutral dimers. This con-

clusion has been corroborated by much recent work on the Na case,[24-29]

$$Na + Na + 2\hbar\omega \rightarrow Na_2^+ + e^- \quad \text{associative ionization}$$

$$Na_2 + 3\hbar\omega \rightarrow Na_2^+ + e^- \quad \text{molecular multiphoton ionization}$$

It has been pointed out[29] that the highly structured components of the dimer–ion spectrum are due to molecular multiphoton ionization, whereas only the broad slowly varying components are due to laser-induced associative ionization. As in the case of the photoassociative laser-induced fluorescence spectra, the broad components can again be explained mainly on the basis of the Franck–Condon principle. In all of the experiments referred to here, only moderate laser powers of less than 10^6 W/cm^2 have been used.

There is, however, one important class of experimental results which cannot be explained on the basis of the Franck–Condon overlap factor: the presence of non-Franck–Condon distributions in the emission spectra of Penning-ionization optical spectroscopy.[30,31] Although to data no such spectral effects have been observed in the intimately related process of associative ionization, there is much theoretical basis to support their presence in such processes.[32,33]

In this article we shall approach the problem of laser/collision-induced bound–free processes from the somewhat specialized vantage point of non-Franck–Condon electronic transitions involving electronic continua. Even though the full impact of such transitions in chemical bond formation is not readily recognized, we hope to convince the reader that a careful study of their origins and effects will lead to some new pathways in the understanding of dissociative and associative events in chemical dynamics. In particular, it will be seen that the laser can be used to its maximum advantage as a controlling agent of chemical bond formation in processes involving such transitions.

In section II we give an overview of the physics behind non-Franck–Condon transitions in bound–free and free–free collisions involving electronic continua, pinpointing their origin to the presence of nonlocal potentials in the nuclear dynamics. As background, we begin by introducing the electronic-field representation as a suitable theoretical tool for the treatment of collision processes in the presence of a laser field. The main physical ideas are then discussed in the context of the gas-phase processes of Penning and associative ionization, with special emphasis on the latter. The presence of special features in the electronic spectrum due to radiative bound–continuum coupling are next introduced. These include the formation of an "extra" discrete electronic state and resonance states. Finally, the discussion is generalized to the case of chemical dynamics on solid surfaces.

Section III focuses on associative ionization. The ideas introduced in section II, such as the breakdown of the Franck–Condon approximation and the nonlocal nuclear potential, are given concrete treatment here. It will be shown in detail how nonlocality actually enhances chemical bond formation and how the laser can be tuned to favor nonlocality.

In section IV, we discuss in detail the spectral features of the "extra" discrete electronic state and resonances, and how these can be exploited for the purpose of creating chemical bonds. As in section III, the discussion is still carried out in the context of collisional ionization. However, as opposed to the processes discussed in section III, where bond formation is mainly achieved through dynamics, it is achieved here mainly through spectroscopy.

The ideas expounded in sections III and IV for gas-phase processes are extended, in a relatively brief fashion, in section V to processes occurring on a solid surface. Here we specialize to low-energy collisions between an impact atom and adsorbate atom and the subsequent capture of the impact atom with the help of a laser. In our discussion, the solid surface is not treated in any realistic fashion—phonons as well as other surface degrees of freedom are ignored. Our objective in introducing the surface is merely to illustrate the wide applicability of the ideas introduced in the previous sections.

While this review constitutes a theoretical treatment of a rather specialized topic in chemical dynamics, we have attempted to maintain a suitable balance between qualitative description on a basic level and detailed mathematical formalism, in the hope that it will be useful to both specialists and nonspecialists alike. The emphasis, however, is always on the physical principles rather than the mathematics. The references cited provide a representative coverage of the literature up to the present.

II. Overview of Laser/Collision-Induced Chemical Bonds Involving Electronic Continua

We shall begin our discussion with Penning and associative ionization. These processes, whether laser-induced or not, differ from many other electronically nonadiabatic collision processes in one important respect: ionization processes necessarily involve an electronic continuum, due to the presence of the liberated electron. Hence, the nuclear collision leading to ionization must be effected by an electronic bound–continuum coupling. Such couplings entail, at least in principle, a nonlocal scattering potential for the collision.[36] Before proceeding to discuss this type of potential, we introduce a general mode of description of potential surfaces especially suitable for laser-induced dynamics, known as the electronic-field representation.[38]

A. The Electronic-Field Representation

This representation is based on the idea of "dressing" molecular quantum states with photon quantum states (in the occupation number or Fock representation). The resulting "dressed" states allow description of collisional and radiative interactions on the same footing and clearly reveal the altered dynamics of a collision system due to the laser. The simplest way to introduce the electronic-field representation is as follows. We begin with a set of potential curves (surfaces) corresponding to different electronic energy levels of the collision system that can be radiatively coupled. Suppose a laser of frequency ω is introduced. All of the curves are shifted by an amount $\hbar\omega$ on the energy scale.

The set of shifted and unshifted curves may cross each other at several nuclear configurations. At every such crossing, radiative coupling is effective and an avoided crossing (level splitting) is generated. These avoided crossings may dramatically change the shapes of the field-free potential curves and thus effectively alter the dynamics of the collision system. The radiatively altered (adiabatic) curves are then called electronic-field curves (surfaces).

B. The Nonlocal Potential and Non-Franck–Condon Spectra

To understand the importance of the nonlocal scattering potential, we first review the basic properties of the local potential. In the context of electronic transitions during an atomic/molecular encounter, a local coupling between different electronic states means that the electronic transitions are effectively "vertical"; i.e., the nuclear configurations remain unchanged during an electronic transition. This can only happen if the electronic motions are much faster than the nuclear ones, so that the electronic transition is completed long before the nuclei have time to change their configurations. This situation then implies that nuclear kinetic energy must be conserved in an electronic transition. For nuclear bound–bound and free–bound transitions, this further implies that the electronic "jump" must occur "instantaneously" and at a specific nuclear configuration. For free–free nuclear transitions, the "jump" can occur at various configurations, but at each one, nuclear kinetic energy must still be conserved.

Intuitively, a nonlocal potential means that an electronic "jump" at a particular nuclear configuration depends on its past and future "history" of "jumps" at all other nuclear configurations. Hence, the probability of such a jump cannot be a local property. Equivalently, it can be imagined that the "jump" takes place over a period of time comparable to the nuclear collision time. Thus the nuclear configuration cannot remain stationary during such a nonlocal electronic transition, and consequently the conservation of nuclear kinetic energy may also be violated in such a process. Yet another way to view the situation is that electronic transitions need not be vertical and the transition spectrum may not be reflected by the Franck–Condon overlap integral. As we shall see in the following sections of this review, this non-Franck–Condon nature of electronic transitions leads to many interesting spectral features, such as the possibility of an increased number of vibrational resonances in the bound AB^+ potential curve.[37] This aspect of the nonlocal coupling obviously has great relevance for the study of laser/collision-induced chemical bonds.

C. "Extra" Electronic Bound State and Resonances

An electronic bound–continuum coupling not only leads to nonlocal nuclear dynamics and the associated non-Franck–Condon behavior of electronic transitions during a nuclear collision, but also makes it possible to create an extra bound (discrete) electronic state which is nonexistent in the absence of the coupling.[39] When this bound–continuum coupling is radiatively generated (e.g., by a laser), it becomes possible to "fine tune" the energy of this bound state by variation of the laser characteristics, such as intensity and frequency. For this bound state to exist, the field intensity must be larger than a certain frequency-dependent critical value. Moreover, multiple metastable states (electronic resonances) not originally present in the field-free spectrum may also be generated by a monochromatic laser. The creation of an extra discrete electronic state enriches the electronic spectrum of the collision complex and thus may conceivably enhance the probability of chemical bond formation. The multiple electronic resonances, on the other hand, with laser-dependent energies and widths, may be yet another cause for the suspected non-Franck–Condon behavior of ionization spectra.

D. Bonds on Solid Surfaces

The effects we have discussed in the previous two subsections are largely due to the presence of an electronic continuum. In gas-phase processes, this continuum is associated mainly with the ionization threshold potential curve (AB^+ in the case of diatomics). In the condensed-phase, however, electronic continuum (bands) are much more common. In particular, the potential surfaces describing the dynamics of adsorbates on solid surfaces many become broadened into bands,[40] and it is expected that nonlocal and other bound–continuum effects discussed earlier would be manifest in collision processes taking place on solid surfaces. Again, a laser can be used to probe various regions of the continuum, and laser-induced molecular collisions on solid surfaces may be a powerful tool for exploring surface structure.

III. Bonds via Dynamics: Laser-Induced Associative Ionization

We first review the basic theory and physical picture behind the processes of field-free Penning and associative ionization,

$$A + B^* \rightarrow A^+ + B + e^- \quad \text{Penning ionization}$$

$$AB^+ + e^- \quad \text{associative ionization}$$

These can be understood in terms of the electronic potential surfaces correlating asymptotically to the atomic fragments A + B* and A^+ + B, as shown in Figure 1. The ionization curve A^+ + B is the lower threshold of an electronic continuum corresponding to the continuous range of energies of the liberated election. Ionization is possible through the collision channel A + B* if its potential curve is embedded in the continuum, as in the case shown in Figure 1, and a configuration interaction bound–continuum coupling is active between the discrete electronic state A + B* and the continuum characterized by the free-electron energy ϵ. This coupling in general depends on both the nuclear configuration R and the electron energy ϵ.

One normally employs the Franck–Condon picture to understand the ionization process. Penning ionization is a nuclear free–free collision. It occurs when the final total energy E_f (electronic plus nuclear) of the collision complex ($E_f = E_i - \epsilon$, where E_i is the initial total

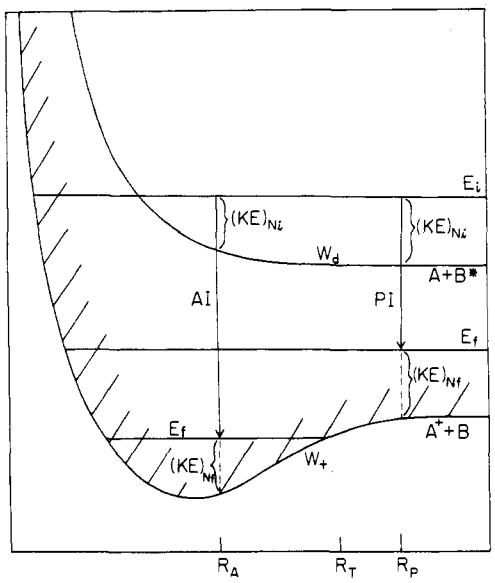

Figure 1. Potential surfaces for Penning and associative ionization. The dashed lines indicate an electronic continuum. E stands for the total energy; $(KE)_N$ stands for the nuclear kinetic energy; the subscripts i and f stand for initial and final. R_p and R_A stand for nuclear configurations where Penning and associative ionization take place, respectively. R_T stands for an approximate transition configuration (see text).

energy) is in the continuous range—larger than $E_{A^+ + B}$ ($R \rightarrow \infty$). The Franck–Condon principle implies that electronic transitions are vertical (nuclear configurations unchanged) and hence the nuclear kinetic energy $(KE)_N$ is conserved,

$$(KE)_{Ni}(R) = (KE)_{Nf}(R) \tag{1}$$

where i and f denote initial and final, respectively. Since E_f is continuous for Penning ionization, the local, vertical electronic transitions between A + B* and A^+ + B can take place in a continuous range of nuclear configurations (R), as long as eq 1 has a solution for R. In Figure 1, for example, all values of $R > \sim R_T$ (T denotes the transition region between Penning and associative ionization) can satisfy eq 1, and hence Penning ionization can take place anywhere in this region. This is reflected by a continuous spectrum of the Penning ionization cross section as a function of the liberated electron energy

$$\epsilon(R) = W_{A+B^*}(R) - W_{A^+ + B}(R) \tag{2}$$

Traditionally this spectrum has been analyzed in terms of the Franck–Condon overlap integral between the continuum (free) nuclear wave functions

$$S(E_i) = \int dR\, \psi^*_{A+B^*}(E_i,R)\psi_{A^+ + B}(E_f,R) \tag{3}$$

This integral depends only on E_i since, by definition,

$$E_f = E_i - \epsilon \tag{4}$$

The situation becomes somewhat different in the associative ionization regime: E_f is quantized here and can only assume discrete values. The Franck–Condon principle, equivalently eq 1, then requires that the bound–continuum transition can only take place at discrete (localized) nuclear configurations. Thus for associative ionization, according to eq 2, the liberated electron can only acquire discretized energies. This is reflected in the resonance structure of the associative part of the ionization spectrum, which is also traditionally analyzed using eq 3. Here E_f is determined largely by the shape of the bound part of the $A^+ + B$ curve, and ionization is most likely to occur at those values of E_i for which $S(E_i)$ is a maximum. By considering the exact nuclear Schrödinger equation describing Penning and associative ionization, it can be shown that[36] the Franck–Condon approximation amounts to replacing an exact nonlocal potential by a local complex one. This local complex potential has the form

$$W(R) = W_d(R) - i\pi|V_{d\epsilon}(R)|^2 \tag{5}$$

where $W_d(R)$ is the potential curve corresponding to the A + B* state, and $V_{d\epsilon}(R)$ is the bound–continuum coupling inducing electronic transitions between $W_d(R)$ and $W_+(R)$ (the curve corresponding to the $A^+ + B$ state) which are ultimately responsible for the ionization process.

Because of this coupling, nuclear dynamics is governed by both the curves $W_d(R)$ and $W_+(R)$. Thus the nuclear Schrödinger equation describing dynamics on $W_d(R)$, for instance, has to contain a part which describes dynamics on $W_+(R)$ also. This part—the propagator function on W_+—is the origin of the nonlocality of the potential. Ignoring complications due to $J \neq 0$ partial waves, the Schrödinger equation for nuclear dynamics on the $W_d(R)$ surface can be written as[36]

$$\left(-\frac{\hbar^2}{2m}\frac{d^2}{dR^2} + W_d(R) - E\right)\chi(E,R) = \int_0^\infty dR'\, V^*_{d\epsilon}(R)V_{d\epsilon}(R')I(E,R,R')\chi(E,R') \tag{6}$$

$$I(E,R,R') = i\pi\left[\int_0^E dE' F(E',R)F^*(E',R') + \sum_v F_v(E_v,R)F_v(E_v,R')\right] \tag{7}$$

where $F(E,R)$ and $F_v(E_v,R)$ are the continuum and bound (vth vibrational level) nuclear wave functions on the potential $W_+(R)$ corresponding to the $A^+ + B$ surface, and it has been assumed that the bound–continuum coupling $V_{d\epsilon}(R)$ is ϵ-independent. Equation 6 clearly involves a nonlocal scattering potential. $I(E,R,R')$ can be understood as the propagator function describing nuclear dynamics on the $W_+(R)$ surface between R and R'. Thus the dynamics at any configuration R depends on the global picture of possible transitions taking place at every other R'. Notice that in eq 7, one can interpret E' as $E' = E - \epsilon$ where ϵ is the energy of the liberated electron. Thus the integral over E' and the summation over E_v is equivalent to an integration over ϵ from 0 to ∞. $E' > E$ would mean negative ϵ, an impossible situation.

Now the Franck–Condon principle of vertical transitions is mathematically equivalent to the following two assumptions: (i) $\chi(E,R')$, the exact wave function in the RHS of eq 6, can be approximated by $\chi_d(E,R')$, the wave function with only $W_d(R)$ as the scattering potential, and (ii) for $E' > E$ the overlap factor $\chi_d(E,R')F^*(E',R')$ leads to a vanishing integral $\int dR'$ on the RHS of eq 6. Under these circumstances the upper limit E in the integral $\int dE'$ for I can be replaced by ∞. From the

assumed completeness of the set of functions $\{F(E,R),F_v(E_v,R)\}$, eq 7 then implies that

$$I(E,R,R') \underset{E\to\infty}{\to} i\pi\delta(R - R') \quad (8)$$

Thus in eq 6 the potential becomes completely local, and is given by eq 5, but $W(R)$ has acquired an imaginary part. A local complex potential means that, even though energy is lost (to the emitted electron), dynamics at each point R is still determined by the local value of $W(R)$. This can only be so if electronic transitions are instantaneous from the viewpoint of nuclear dynamics, a requirement of the Franck–Condon approximation.

The implication of eq 6 and 7 is clear: the scattering potential for nuclear dynamics on $W_d(R)$ only becomes rigorously local in the high-energy limit $E \to \infty$. Nonlocality increases in importance as the collision energy is reduced, and when $E < W_+(\infty)$ the nonlocal part of the imaginary part of the potential becomes dominant.[36] In practice, of course, as $E \to \infty$, nuclear and electronic time scales become equivalent and the breakdown of the Born–Oppenheimer approximation will render the Franck–Condon approximation meaningless. Thus the Franck–Condon approximation can only be expected to hold in a certain intermediate collision-energy range—not so large such that nuclei and electrons move with comparable velocities and yet not so small such that nonlocal potentials governing nuclear motion become important.

A. Pictorial Interpretation of the Nonlocal Potential

The physics of the nonlocal potential is contained in the propagator $I(E,R,R')$ given by eq 7. To obtain a pictorial interpretation of this quantity, it is instructive to write down the formal solution for eq 6 in a Born series. First we convert the integrodifferential equation 6 into an integral equation,

$$\chi(E,R) = \chi_d(E,R) + \int_0^\infty dR'\, G(E,R,R')V_{d\epsilon}^*(R') \times \int_0^\infty dR''\, V_{d\epsilon}(R'')I(E,R',R'')\chi(E,R'') \quad (9)$$

where $G(E,R,R'')$ is the Green's function or propagator on the $W_d(R)$ surface,

$$G(E,R,R'') = \int_0^\infty dE' \frac{\chi_d^*(E',R)\chi_d(E',R')}{E - E'} \quad (10)$$

and $\chi_d(E,R)$ is the wave function for scattering on the surface $W_d(R)$ alone; i.e., it satisfies the homogeneous part of eq 6,

$$\left\{-\frac{\hbar^2}{2m}\frac{d^2}{dR^2} + W_d(R) - E\right\}\chi_d(E,R) = 0 \quad (11)$$

The Born series is then obtained from eq 9 by iteration. The lowest order (Born approximation) is given by

$$\chi^{(1)}(E,R) = \chi_d(E,R) + \int_0^\infty dR'\, G(E,R,R')V_{d\epsilon}^*(R') \times \int_0^\infty dR''\, V_{d\epsilon}(R'')I(E,E',R'')\chi_d(E,R'') \quad (12)$$

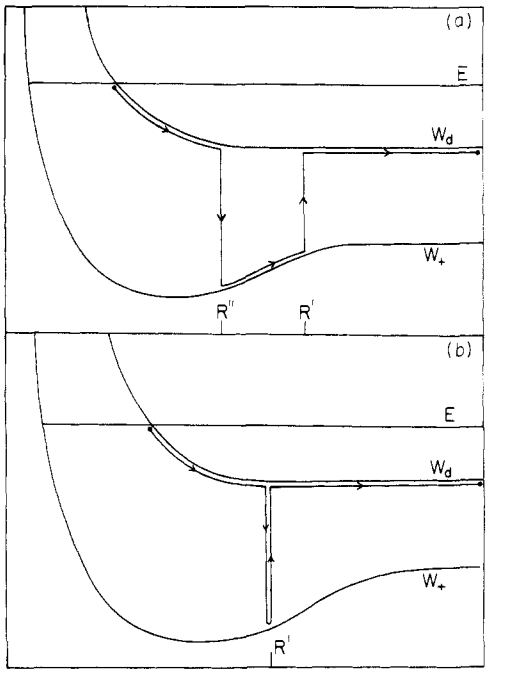

Figure 2. Pictorial representations of first-order nonlocal (a) and local (Franck–Condon vertical) transitions (b) (see eq 12 and 13).

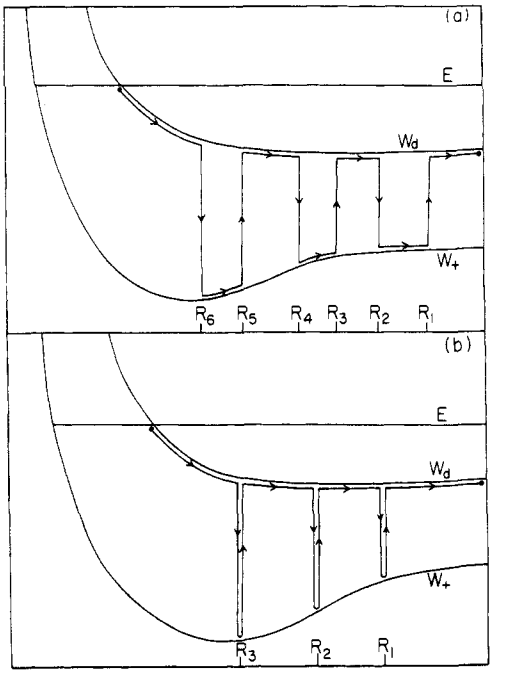

Figure 3. Pictorial representations of third-order nonlocal (a) and local (Franck–Condon) transitions (b).

which can be contrasted with the Born approximation using the local complex potential $W(R)$ [eq 5],

$$\chi^{(1)}(E,R) = \chi_d(E,R) + i\pi\int_0^\infty dR'\, G(E,R,R')|V_{d\epsilon}(R')|^2\chi_d(E,R') \quad (13)$$

The physical picture represented by these equations is illustrated in Figure 2, parts a and b, respectively. In these figures, propagation on the upper surface $W_d(R)$ corresponds mathematically to the propagator $G(E,R,R')$, whereas that on the lower surface $W_+(R)$ to the propagator $I(E,R,R')$. The bound–continuum coupling $V_{d\epsilon}(R)$ induces a "kick" from the upper to the lower

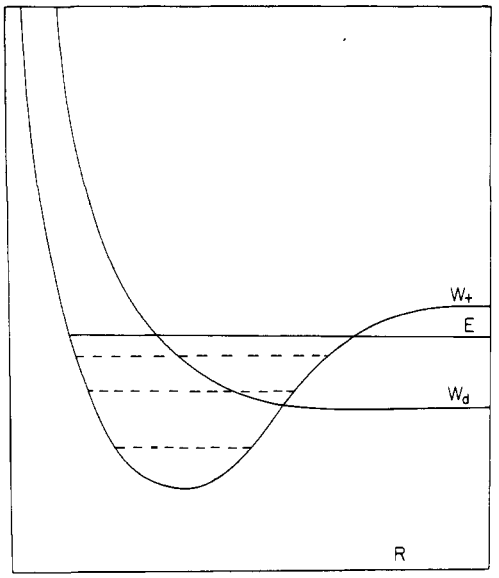

Figure 4. A situation in which associative ionization and nonlocal dynamics are predominant, characterized by $E < W_+(\infty)$. Dashed lines represent vibrational levels.

surface at R, and $V_{d\epsilon}^*(R)$ does the reverse. It is clear from Figure 2 that a nonlocal potential allows the system to "live" for a finite period of time on the $W_+(R)$ surface and thus enhances ionization, whereas a local potential only allows for momentary existence on that surface. Also, the local picture clearly implies the Franck–Condon principle of vertical electronic transitions, whereas the nonlocal picture apparently allows for nonvertical transitions.

It is straightforward to generalize the picture to higher orders in the Born series. For example, a third-order process (involving six transitions) is shown in Figure 3. In both Figures 2 and 3, all the marked coordinates are arbitrary and hence have to be integrated over. Thus in Figure 3a, it is possible for $R_1 = R_2$, $R_3 = R_4$, and $R_5 = R_6$. Hence, the local picture is only a very specialized case of the nonlocal one.

In view of Figures 2 and 3, it can also be understood intuitively why, as $E \rightarrow \infty$, the potential becomes progressively more local. Indeed, as the collision energy increases, the transit (interaction) time for the collision decreases, and it becomes increasingly more difficult to effect a transition of the type shown in Figure 2a, involving a finite duration of time on the lower surface. Correspondingly, transitions of the type shown in Figure 2b, involving zero time in the lower surface, become more favored. Conversely, low collision energies, implying large interaction times, favor the nonlocal processes. Since, as observed above, nonlocal transitions enhance ionization, low-energy collisions should also favor ionization. In particular, if the energy is so low that $E < W_+(\infty)$, as shown in Figure 4, then only associative ionization occurs. In this case it can be shown that[36] the dispersive (imaginary) part of the potential is entirely nonlocal and the propagator $I(E,R,R')$ in eq 7 only involves bound vibrational wave functions $F_v(E,R)$ for the potential $W_+(R)$,

$$I(E,R,R') \overset{AI}{\rightarrow} \sum F_v(E_v,R)F_v(E_v,R') \qquad (14)$$

where the sum is only over the vibrational states that are energetically accessible for a given E.

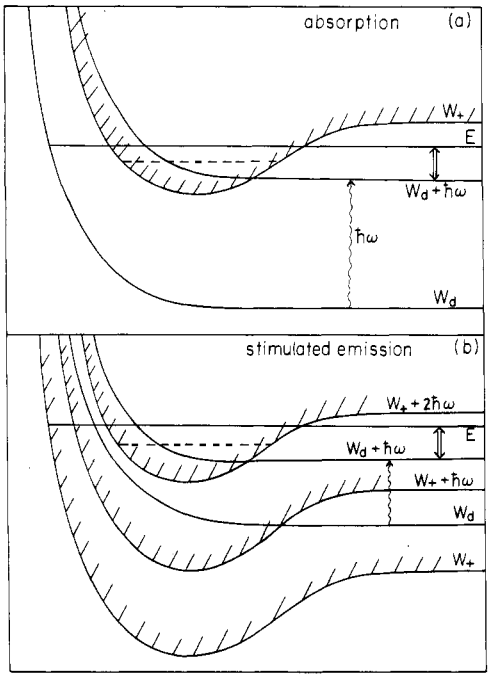

Figure 5. Laser selection of collision energies in associative ionization through (a) absorption and (b) stimulated emission. The double arrows represent the laser-selected nuclear kinetic energies on the entrance channels.

B. Laser Selection of Collision Energy by Absorption and Stimulated Emission of Photons

Rather than varying the collision energy with respect to fixed potential curves on the energy scale, one can use a laser to change the relative positions of the potential curves and thus the effective collision energy in the entrance channel. This can be done by tuning the laser frequency ω and is most easily seen using the electronic-field representation for the field-dressed electronic states, as discussed earlier. Figure 5, parts a and b, illustrates two situations for laser-enhanced associative ionization, which are equivalent dynamically, but arise from distinct radiative mechanisms. Figure 5a shows ionization through photon absorption, whereas Figure 5b shows ionization through stimulated emission. For the absorption case, associative ionization does not occur without the laser, since $W_d(R) < W_+(R)$ for all R. For the stimulated emission case, field-free associative ionization may occur but is much enhanced by the presence of the laser. For absorption, the electronic transition takes place between the electronic-field curves $W_d + \hbar\omega \rightarrow W_+$; for emission, the transition is $W_d + \hbar\omega \rightarrow W_+ + 2\hbar\omega$. (We recall that for stimulated emission, the incident photon is not absorbed, and in the final state another photon of the same mode is deposited into the radiation field.) Since nuclear dynamics takes place on these curves, it is seen that Figure 5, parts a and b, represents qualitatively dynamically equivalent cases. For both situations the initial kinetic energy on the entrance channel,

$$(KE)_i = E - (W_d + \hbar\omega) \qquad (15)$$

is represented by the double-arrow. Dashed lines represent vibrational levels supported by the bound parts of the W_+ ionization threshold curves.

Figure 5, parts a and b clearly shows that one can

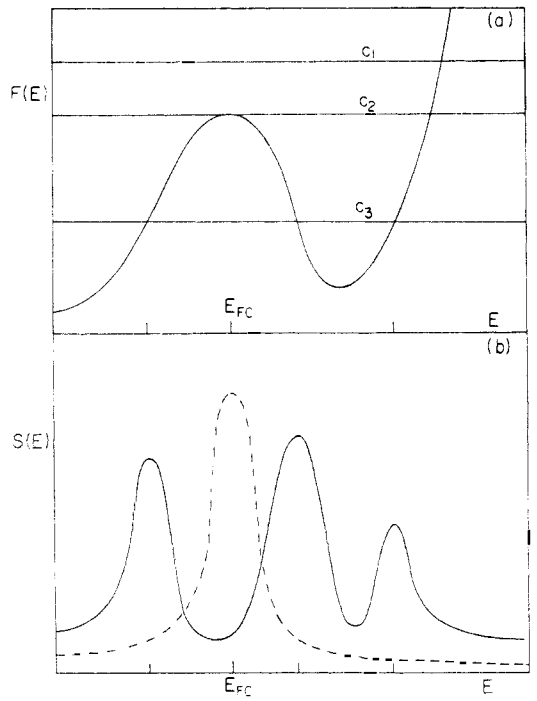

Figure 6. (a) Qualitative picture of a Franck–Condon overlap function in the neighborhood of a local maximum. C_i (i = 1, 2, 3,) are three values of C (eq 21) corresponding to three laser intensities (C_1 corresponds to the smallest and C_3 the largest). E_{FC} is the Franck–Condon resonance energy. (b) Qualitative picture for the associative ionization (resonance) spectrum. The dashed curve represents the Franck–Condon result; the solid curves show multiple resonances due to nonlocality.

fine-tune the laser frequency to "energy-select" the collision partners to access the desired regions of the bound vibrational wells in W_+. Furthermore, from our previous discussion, one can decrease $(KE)_i$ to accentuate the nonlocal effects and thus enhance the overall formation of the A–B bond.

C. Multiple Vibrational Resonances

This enhancement due to nonlocal effects basically arises from the physical picture of Figures 2a and 3a: the collision system can "live" longer on the $W_+(R)$ curve. In the Franck–Condon picture (Figures 2b and 3b) it is expected that for the vibrational level E_v in W_+, interference between the amplitudes corresponding to different numbers of "instantaneous transitions" would lead to one resonance energy E favoring associative ionization. The corresponding resonant electron energy ϵ is given by

$$\epsilon = E - E_v \tag{16}$$

In the nonlocal picture (Figures 2a and 3a), on the other hand, interference between amplitudes corresponding to different numbers of "finite-time transitions" may lead to more than one vibrational resonance energy E favoring associative ionization for a single vibrational level.[37] This can be seen qualitatively from the nonlocal picture: a net downward transition involving a finite "lifetime" in W_+ no longer corresponds to fixed ϵ. Thus in eq 16 E is no longer unique for a fixed vibrational level.

Restricting our attention to a single vibrational level for simplicity, with wave function $F_0(E_0,R)$ (cf. eq 6), eq 14 for $I(E,R,R')$ reduces to a single term. Equation 5 can then be solved analytically since in the RHS of that equation, the sum of nonlocal potentials reduces to a single nonlocal potential with a separable kernel. The solution is given by[37]

$$\chi(E,R) = \phi_0(E,R) + \frac{i\pi\mathcal{F}(E)}{1 - i\pi Y(E)} \times \int_0^\infty dR'\, G(E;R,R')V_{d\epsilon}^*(R')F_0(E_0,R') \tag{17}$$

where

$$\mathcal{F}(E) \equiv \int_0^\infty dR\; V_{d\epsilon}(R)F_0(E_0,R)\chi_d(E,R) \tag{18}$$

is the generalized Franck–Condon overlap integral, and

$$Y(E) \equiv \mathbf{p}\int_0^\infty dE' \frac{|\mathcal{F}(E)|^2}{E - E'} - i\pi|\mathcal{F}(E)|^2 \tag{19}$$

Since we can assume that the Green's function $G(E,R,R')$ has no bound-state poles, the resonance energies E can be determined by setting the real part of the denominator in eq 17 equal to zero,

$$1 - \pi^2|\mathcal{F}(E)|^2 = 0 \tag{20}$$

This is an interesting result. If we assume that $V_{d\epsilon}(R)$ is independent of R, eq 20 can be written as

$$|F(E)|^2 = \frac{1}{\pi^2|V_{d\epsilon}|^2} \equiv C \tag{21}$$

where $F(E)$ is the usual Franck–Condon overlap

$$F(E) \equiv \int_0^\infty dR\; F_0(E_0,R)\chi_d(E,R) \tag{22}$$

Thus in the nonlocal case the resonance collision energies are not determined by the maximum of the Franck–Condon overlap, as required by the Franck–Condon principle, but by eq 21.

For a laser-induced process (Figure 5), we not only can vary E by changing the laser frequency, but also control the resonance energy by varying the laser intensity, which governs $V_{d\epsilon}$. This situation can be understood with the help of Figure 6. Figure 6a shows a qualitative picture of a Franck–Condon overlap function in the neighborhood of a local maximum. The three values C_1, C_2, and C_3 (eq 21) correspond to three bound–continuum coupling strengths $V_{d\epsilon}$, with the largest $V_{d\epsilon}$ for C_3 and the smallest for C_1. It is clear that for $V_{d\epsilon}$ larger than a certain critical value, multiple resonances can occur. Figure 6b shows a qualitative picture for the resonance spectrum $S(E)$ according to the Franck–Condon principle (dashed curve) and to the result of eq 21 due to a nonlocal potential (solid curve). It is seen that a nonlocal potential may either shift a "pure" Franck–Condon spectrum or split it into multiple components. For laser-induced processes where $V_{d\epsilon}$ is due to electric-dipole coupling, $V_{d\epsilon} \sim \mu_0\mathcal{E}/(\hbar\omega_0)^{1/2}$ where μ_0 is the electric dipole of the A + B system, $\mathcal{E}$ is the electric field strength of the laser, and ω_0 is the natural frequency of the bound vibrational mode supported by W_+. We have shown elsewhere[37] that the critical dimensionless coupling constant $V_{d\epsilon}^2/\hbar\omega_0$ for multiple resonance formation (corresponding to C_2 in Figure 6a) is on the order of 0.5. Using the typical values $\mu_0 \sim 10$ au and $\omega_0 \sim 120$ cm^{-1}, it can then be

estimated that the critical laser power for multiple resonance formation is on the order of 10^6–10^7 W/cm^2.

IV. Bonds via Spectroscopy

Non-Franck–Condon spectra arising from electronic bound-continuum processes can also be understood in terms of spectral, as opposed to dynamical, effects due to nonlocal potentials. In laser-induced processes, the radiative bound–continuum coupling can be readily manipulated by varying the laser characteristics to produce many novel spectral features in a given system. Very interesting studies have recently been carried out on the general aspects of this problem[39] and the specific atomic processes of laser-induced autoionization[41-45] and photodetachment of electrons from negative ions.[46-49] In this section, we shall discuss these spectral features in the context of molecular dynamics and indicate how they can be exploited for the purpose of bond formation.

A. Laser-Induced Electronic Resonances and the Renormalized Width

Electronic resonances play a crucial role in atomic dissociation and recombination events. Their properties for field-free processes such as electron–molecule scattering have been dealt with exhaustively using the analytic properties of the associated S-matrices.[50] Here we examine their role in nuclear dynamics with reference to bond formation.

In the previous section, nuclear dynamics is governed by the potential surfaces $W_d(R)$ and $W_+(R)$, which label the corresponding electronic states $|\phi_d,R\rangle\rangle$ and $|\phi_\epsilon,R\rangle\rangle$. (Double brackets are used because separate Hilbert spaces are needed to describe the two different kinds of degrees of freedom, the electronic (r) and the internuclear (R).) Since $|\phi_d,R\rangle\rangle$ and $|\phi_\epsilon,R\rangle\rangle$ are coupled electronically, they are called states in the diabatic representation. $V_{d\epsilon}(R)$ then represents the off-diagonal matrix elements of the electronic Hamiltonian in this representation. To study the electronic spectrum in detail, one needs to use the adiabatic representation, in which the electronic hamiltonian is diagonalized. From now on we shall denote the diabatic states simply by the single bracket, $|\phi_d\rangle$ and $|\phi_\epsilon\rangle$, where R is regarded as a parameter and is omitted. The adiabatic states $|E\rangle$ with energy E are then defined by

$$H_{el}|E\rangle = E|E\rangle \tag{23}$$

where H_{el} is the electronic Hamiltonian. $|E\rangle$ can be expanded in terms of the diabatic states,

$$|E\rangle = \beta_E|\phi_d\rangle + \int d\epsilon\, \rho(\epsilon)\, \chi_{E\epsilon}|\phi_\epsilon\rangle \tag{24}$$

where $\rho(\epsilon)$ is an appropriate density of states in the continuum, and the expansion coefficienty β_E and $\chi_{E\epsilon}$ both depend on the bound–continuum coupling

$$V_{d\epsilon}(R) = \langle\phi_\epsilon|H_{el}|\phi_d\rangle \tag{25}$$

The eigenvalue equation for H_{el} follows from eq 23,

$$E - W_d(R) + \int_\mu^\infty d\epsilon\, \frac{\rho(\epsilon)|V_{d\epsilon}|^2}{\epsilon - E} = 0 \tag{26}$$

where μ is the continuum threshold. Equation 26 implies that electronic resonances may occur provided that the equation

$$E - W_d + \mathbf{p}\int_\mu^\infty d\epsilon\, \frac{\rho(\epsilon)|V_{d\epsilon}|^2}{\epsilon - E} = 0 \tag{27}$$

has solutions for $E > \mu$. In traditional work the principal-value integral in eq 27 is usually interpreted as a small shift to the line center W_d. However, when $V_{d\epsilon}$ varies significantly over a region ϵ of interest, such as in the case of radiative couplings, this treatment becomes invalid. In such a case eq 27 may have multiple solutions, which bear no simple relationship to W_d.[39] These can be identified as electronic resonances corresponding to complex adiabatic potential surfaces. Just as in the localized potential treatment of nuclear dynamics in the diabatic representation, where the appropriate complex potential surface is given by eq 8, in the adiabatic representation nuclear dynamics occurs on the adiabatic complex potential surfaces

$$W_A(R) = E_r(R) - i\frac{\Gamma(R)}{2} \tag{28}$$

where E_r is a resonance energy at the internuclear distance R (a solution to eq 27) and $\Gamma(R)$ represents the width. There are now two complications. First, for fixed R, these may be more than one value of E_r (multiple resonances). Second, the width $\Gamma(R)$ is not proportional to the square of the "bare" coupling strength, $|V_{d\epsilon}|^2$, but to the square of a renormalized coupling strength,[39]

$$\Gamma(E_r) = \frac{\Gamma_0(E_r)}{1 + P'(E_r)} \tag{29}$$

where

$$P'(E_r) \equiv \frac{d}{dE}\left\{\int d\epsilon\, \frac{\rho(\epsilon)|V_{d\epsilon}(R)|^2}{\epsilon - E}\right\}_{E = E_r} \tag{30}$$

and $\Gamma_0(E)$ is the bare width given by

$$\Gamma_0(E) \equiv 2\pi\rho(E)|V_{dE}(R)|^2 \tag{31}$$

It is interesting to note the situation when $V_{d\epsilon}$ is due to the radiative coupling induced by a laser, in which case $V_{d\epsilon}$ becomes adjustable. The width Γ is then not proportional to the physical field intensity, but to a "renormalized" field intensity which depends on the resonance energy E_r. According to eq 29, provided $P'(E_r) > 0$, Γ is always less than Γ_0. Thus, the range of values of E for which $P'(E) > 0$ may be considered as the metastable regime: if a resonance state has energy E_R within this regime, its physical width is always smaller than its bare width. In this sense, a laser, in addition to creating a resonance state, may actually enhance the stability of that state. For $-1 < P' < 0$, Γ is still positive, but it is larger than Γ_0. The range of E satisfying this inequality may be called the unstable regime, as Γ can become very large when $P' \gtrsim -1$. In this regime, a laser destabilizes a resonance state that it creates. Finally, for $P' < -1$, $\Gamma(E_r)$ becomes negative, and the solutions of eq 27 do not correspond to any physically observed resonances at all. Hence, we can label the range of E satisfying this condition as the unphysical regime.

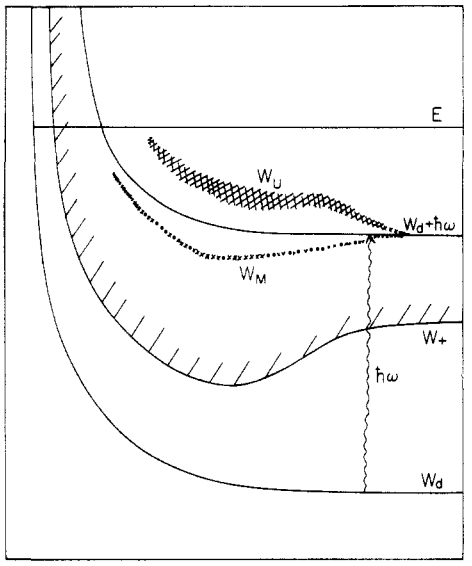

Figure 7. Complex potential surfaces (with renormalized widths) corresponding to laser-induced electronic resonances. The upper curve, W_U, is in the unstable regime, and the lower curve, W_M, is in the metastable regime. It is assumed that the radiative coupling is insignificant at asymptotic regions so that no splitting occurs there.

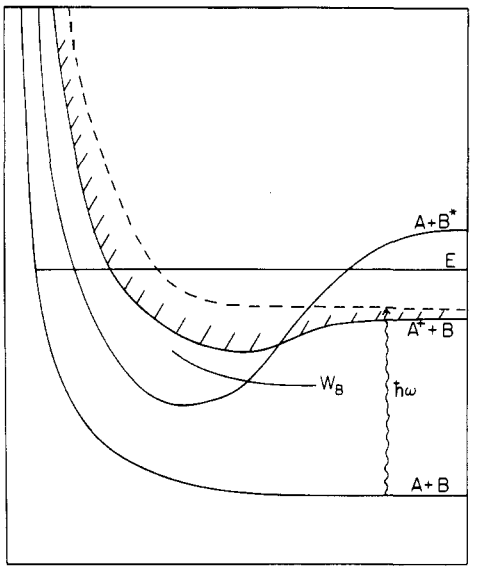

Figure 8. Indirect laser/collision-induced preassociation via the ionization channel. The radiative coupling indicated by the wiggly photon line is forbidden. W_B is the potential curve corresponding to the laser-induced electronic discrete state.

In the context of collisional ionization, resonance states in the metastable regime inhibit ionization, those in the unstable regime enhance ionization, and finally, the unphysical regime prohibits ionization altogether. Figure 7 represents schematically the situation for an absorption process. In this case, the bare state $W_d + \hbar\omega$ splits up into two resonance states due to radiative coupling. The one above $W_d + \hbar\omega$, W_U, is in the unstable regime, where as the one below $W_d + \hbar\omega$, W_M, is in the metastable regime. Semiclassically, one can then view nuclear dynamics as taking place on both of these "resonance" potential surfaces. The trajectory on W_U will favor ionization. This situation should be reflected in a departure from a pure Franck–Condon behavior of the ionization spectrum.

B. Laser-Induced Electronic Discrete States: Neutral Preassociation via the Ionizing Channel

So far we have only examined the solutions of eq 26 for $E > \mu$. A solution below the continuum threshold ($E < \mu$), however, can exist provided

$$\int_{\mu}^{\infty} d\epsilon \frac{\rho(\epsilon)|V_{d\epsilon}|^2}{\epsilon - \mu} > W_d - \mu \tag{32}$$

This implies that a discrete electronic state with energy below the ionization threshold can be induced by a laser, provided the laser intensity is larger than a certain critical value. In the context of Figure 7, eq 32 is equivalent to the following equation for a critical laser intensity,

$$I_C(R) = \frac{\hbar\omega - [W_+(R) - W_d(R)]}{\int_{W_+}^{\infty} d\epsilon \frac{\rho(\epsilon)|\mathcal{V}(\epsilon)|^2}{\epsilon - W_+}} \tag{33}$$

such that a discrete electronic potential curve will be created for $I > I_C$. In eq 33 we have made use of the fact that $|V_{d\epsilon}|^2 \propto$ laser intensity I and have written

$$|V_{d\epsilon}|^2 \equiv I|\mathcal{V}(\epsilon)|^2 \tag{34}$$

For fixed laser frequency, the potential curves in Figure 7 result if $I < I_C$. As I is increased, the resonance states become more separated with W_U becoming more unstable and W_M more stable. Thus, as the intensity of the laser is increased, the latter has the effect of "pulling down" the energy level of the induced metastable resonance state and stabilizing it more in the process. As the intensity is increased beyond I_C, the resonance state gets "pulled" out of the continuum and becomes a truly bound electronic potential surface, $W_B(R)$.

To estimate I_c we need to assume specific forms for $V_{d\epsilon}$ and $\rho(\epsilon)$. By use of the typical forms[39]

$$\rho(\epsilon) = \alpha\sqrt{\epsilon - W_+} \tag{35}$$

and

$$|V_{d\epsilon}|^2 = \frac{\gamma^4}{(\epsilon - \epsilon_0)^2 + \xi^2} \tag{36}$$

where α, γ, ϵ_0 ($> W_+$), and ξ are constants, the integral in eq 32 can be evaluated[39] and eq 32 can be rewritten as

$$(\alpha\gamma^4)_c = \frac{\xi[\hbar\omega + W_d - W_+][(\epsilon_0 - W_+)^2 + \xi^2]^{3/4}}{\pi\left[(\epsilon_0 - W_+)\cos\frac{\theta}{2} + \xi\sin\frac{\theta}{2}\right]} \tag{37}$$

where $(\alpha\gamma^4)_c$ [of dimensions (energy)$^{5/2}$] is the critical coupling constant for the formation of W_B. Thus for electric-dipole coupling $(\alpha\gamma^4)_c \sim (\mu_0\mathcal{E}_c)^{5/2}$, where μ_0 is the electric dipole of the molecular collision system and $\mathcal{E}_c$ is the critical laser field strength. Equation 37 can be simplified to give a rough estimate for $\mathcal{E}_c$ if we make

the plausible approximations that $\epsilon_0 \sim W_d + \hbar\omega$ and $\xi \sim W_d + \hbar\omega - W_+$:

$$\mathcal{E}_c \sim \frac{0.7}{\mu_0}(W_d + \hbar\omega - W_+) \quad (38)$$

Assuming a typical choice for $W_d + \hbar\omega - W_+ \sim$ of 5×10^{-4} au, I_c is then estimated to be 10^6–10^7 W/cm^2, similar to the intensities required for multiple resonance formation in associative ionization.

In Figure 8, we illustrate an interesting dynamical consequence of this laser-induced discrete surface. This figure shows a possible mechanism for the associative process

$$A + B \rightarrow AB^* \quad (39)$$

which is not possible through either pure collision or a direct process of collision with photon absorption. The latter is ruled out on the basis of the assumption that neither the finite nuclear distance nor asymptotic electronic states corresponding to the surfaces for A + B* and A + B can be radiatively coupled to a significant extent. These states can, however, be indirectly coupled through the ionization channel $A^+ + B$, provided the laser intensity is high enough such that an electronically discrete surface crossing the A + B* bound well is induced. Notice that, as discussed above, the existence of W_B and unstable resonances within the continuum are mutually exclusive, so that the ionization channel will not be a competitive channel to association. Also, W_B need not exist as a complete potential surface, and is consequently not shown as such in the figure. All that is required is that there is a portion which crosses the bound A + B* well. We call this process laser- and collision-induced preassociation via the ionization channel. In this scenario, the laser becomes a truly versatile tool when used in conjunction with a collision process. It can "turn on" ionization when $I < I_C$ and can "turn off" ionization when $I > I_C$. In the latter case, the induced electronic discrete potential surface W_B provides a bridge to access other electronic states. Another important advantage is that the laser frequency is not critical, in sharp contrast to many laser-induced processes. All that is required is that some part of the continuum be accessed.

V. Bonds on Solid Surfaces

The electronic-field picture for describing gas-phase atomic/molecular collisions involving an electronic continuum discussed in the previous sections can be generalized to the description of collision processes taking place on a solid surface. In the presence of a surface, the electronic continuum arises from the periodic lattice structure of the substrate, but the qualitative description of the nuclear dynamics can be carried over from the gas-phase situation. Much interesting theoretical work has been carried out by using this approach on the problem of electron-stimulated desorption.[51-53] Here we shall use it to briefly discuss a laser-induced atom–adsorbate collision process.

In Figure 9, A represents an adsorbate atom and B* an impact atom colliding with A. A laser with a suitable frequency ω is also incident on the system. The potential curves are similar to those in Figure 1, where the bottom curve now represents the ground electronic state

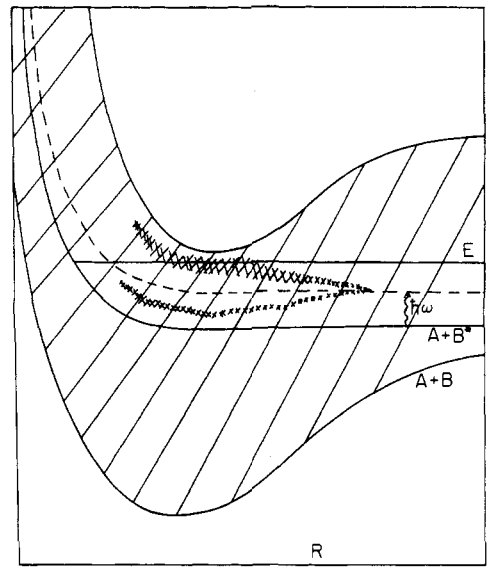

Figure 9. Laser-induced energy transfer from an excited atom B* (colliding with adsorbate A) to the electronic continuum (shaded) resulting in possible bond formation between A and B. The hatched areas represent laser-induced electronic resonances.

of the A + B system. The electronic continuum, now describing an A-surface electronic band, need not extend to infinite energy. The qualitative features of the dynamics, however, remain unchanged if the A + B* curves is still partly or wholly embedded in the band. The laser can be used to transfer the excitation energy from B* into the electronic continuum, so that a bound collision complex results. R represents the relevant A–B collision coordinate, and the lattice coordinates of the solid are considered to be frozen so that energy transfer to phonons of the solid are ignored.

Energy transfer resulting in a bound complex can again take place in two ways: photon absorption and stimulated emission. Figure 9 illustrates the absorption mechanism (compare with Figure 7). The radiative coupling generated by the laser between the electronically excited state A + B* and the A + B band may create a broad resonance in the unstable regime of the band and a narrow resonance in the metastable regime (see the theoretical discussion in the previous section). If, as shown in the figure, the broad resonance has higher energy, then it will contribute more significantly to nuclear dynamics in comparison to the lower energy narrow resonance curve. This is simply because the nuclear kinetic energy is smaller on the broad resonance curve, and more time will be spent there by the system in a collision encounter. Thus, the laser has created a favorable situation for energy transfer to the continuum and possible relaxation to the bound AB state. The stimulated emission mechanism can be illustrated by Figure 5b, with W_+ representing the A + B state and W_d the A + B* state. In this case, the electronic energy transfer induced by the laser may lead to multiple resonances for the nuclear motion. As in the gas-phase scenario, this is due to nonlocal dynamical effects arising from the bound–continuum electronic coupling.

One difference between processes on a solid surface and the corresponding gas-phase processes is that the former only involve a finite-width continuum. The finite bandwidth of the continuum in general makes it

less "usable" for the purpose of energy transfer and makes the dynamics much more system-dependent. Nevertheless, the qualitative features of the theory presented for the gas-phase case in the previous section are still valid. A more complete picture will obviously involve electron–phonon and photon–phonon interactions. These fall outside the scope of the present article.

VI. Acknowledgments

This research was supported in part by the National Science Foundation under Grant CHE-8519053 and the Air Force Office of Scientific Research (AFSC), United States Air Force, under Contract F49620-86-C-0009.

VII. References

(1) For a review of the field up to 1984, see, for example: George, T. F.; Beri, A. C.; Lam, K. S.; Lin, J. T. In *Laser Applications*; Ready, J. F., Erf, R. K., Eds.; Academic: New York, 1984; Vol. 5, p 69, and references contained therein.
(2) See, for example: George, T. F. *Opt. Eng.* **1979**, *18*, 167.
(3) Falcone, R. W.; Green, W. R.; White, J. C.; Young, J. E.; Harris, S. E. *Phys. Rev. A* **1977**, *15*, 1333.
(4) Cahuzac, P.; Toschek, P. E. *Phys. Rev. Lett.* **1978**, *40*, 1087.
(5) Green, W. R.; Lukasik, J.; Willison, J. R.; Wright, M. D.; Young, J. F.; Harris, S. E. *Phys. Rev. Lett.* **1979**, *42*, 970.
(6) Hering, P.; Brooks, P. R.; Curl, R. F., Jr.; Judson, R. S.; Lowe, R. S. *Phys. Rev. Lett.* **1980**, *44*, 687.
(7) Bonch-Bruevich, A. M.; Vartanyan, T. A.; Khromov, V. V. *Zh. Eksp. Teor. Fiz.* **1980**, *78*, 583; *Sov. Phys. JETP (Engl. Transl.)* **1980**, *51*, 271.
(8) Kleiber, P. D.; Burnett, K.; Cooper, J. *Phys. Rev. Lett.* **1981**, *47*, 1595.
(9) Wilcomb, B. E.; Burnham, R. E. *J. Chem. Phys.* **1981**, *74*, 6784.
(10) Lukasik, J.; Wallace, S. C. *Phys. Rev. Lett.* **1981**, *47*, 240.
(11) Pillet, P.; Kachru, R.; Tran, N. J.; Smith, W. W.; Gallagher, T. F. *Phys. Rev. Lett.* **1983**, *50*, 1763.
(12) Ku, J. K.; Inuoe, G.; Setser, D. W. *J. Phys. Chem.* **1983**, *87*, 2989.
(13) Sizer, Theodore, II; Raymer, M. G. *Phys. Rev. Lett.* **1986**, *56*, 123.
(14) Hutchinson, M.; George, T. F. *J. Phys. Chem.* **1983**, *87*, 2037.
(15) Shapiro, M.; Brumer, P., manuscript in preparation.
(16) Schmidt, C. *Chem. Phys. Lett.* **1976**, *37*, 574.
(17) Bandrauk, A. D.; Sink, M. L. *Chem. Phys. Lett.* **1978**, *57*, 569; *J. Chem. Phys.* **1981**, *74*, 1110.
(18) Milfeld, K. F.; Bowman, J. M. *Chem. Phys. Lett.* **1983**, *100*, 529.
(19) Saha, H. P.; Dahler, J. S.; Jones, D. M. *Phys. Rev. A* **1984**, *30*, 1345.
(20) Ehrlich, D. J.; Osgood, R. M., Jr. *Phys. Rev. Lett.* **1978**, *41*, 547; *IEEE J. Quantum Electron.* **1979**, *QE-15*, 301.
(21) Inoue, G.; Ku, J. K.; Setser, D. W. *J. Chem. Phys.* **1982**, *76*, 733; *J. Chem. Phys.* **1984**, *80*, 6006.
(22) Ehrlich, D. J.; Osgood, R. M., Jr. *J. Chem. Phys.* **1980**, *73*, 3038.
(23) Boulmer, J.; Weiner, J. *Phys. Rev. A* **1983**, *27*, 2817.
(24) Polak-Dingels, P.; Delpech, J.-F.; Weiner, J. *Phys. Rev. Lett.* **1980**, *44*, 1663.
(25) Weiner, J.; Polak-Dingels, P. *J. Chem. Phys.* **1981**, *74*, 508.
(26) Carrē, B.; Roussel, R.; Breger, P.; Spiess, G. *J. Phys. B* **1981**, *14*, 4271.
(27) Allegrini, M.; Garver, W. P.; Kushawaha, V. S.; Leventhal, J. J. *Phys. Rev. A* **1983**, *28*, 199.
(28) Burkhardt, C. E.; Garver, W. P.; Kushawaha, V. S.; Leventhal, J. J. *Phys. Rev. A* **1984**, *30*, 652.
(29) Keller, J.; Weiner, J. *Phys. Rev. A* **1984**, *30*, 213.
(30) Robertson, W. W. *J. Chem. Phys.* **1966**, *44*, 2456.
(31) Richardson, W. C.; Setser, D. W.; Albritton, D. L.; Schmeltekopf, A. L. *Chem. Phys. Lett.* **1971**, *12*, 349.
(32) O'Malley, T. F. *Phys. Rev.* **1966**, *150*, 14.
(33) Nakamura, H. *J. Phys. Soc. Jpn.* **1968**, *24*, 1353; **1969**, *26*, 1473.
(34) Bieniek, R. J. *Phys. Rev. A* **1978**, *18*, 392; *J. Phys. B* **1980**, *13*, 4405; **1981**, *14*, 1707.
(35) Lam, K. S.; George, T. F. *J. Phys. Chem.* **1983**, *87*, 2799.
(36) Lam, K. S.; George, T. F. *Phys. Rev. A* **1984**, *29*, 492.
(37) Lam, K. S.; George, T. F. *Phys. Rev. A* **1985**, *32*, 1650.
(38) George, T. F.; Zimmerman, I. H.; Yuan, J. M.; Laing, J. R.; Devries, P. L. *Acc. Chem. Res.* **1977**, *10*, 449.
(39) Lam, K. S.; George, T. F. *Phys. Rev. A* **1986**, *33*, 2491.
(40) For a review of adsorption on metal surfaces, see, for example: Muscat, J. P.; Newns, D. M. *Prog. Surf. Sci.* **1978**, *9*, 1. Gadzuk, J. W. In *Atomistics of Fracture*; Latanision, R. M.; Pickens, J. R., Eds.; Plenum: New York; p 391.
(41) Lambropoulos, P.; Zoller, P. *Phys. Rev. A* **1981**, *24*, 379.
(42) Rzażewski, K.; Eberly, J. H. *Phys. Rev. A* **1983**, *27*, 2026.
(43) Haus, J. W.; Lewenstein, M.; Rzazewski, K. *Phys. Rev. A* **1983**, *28*, 2269.
(44) Haan, S. L.; Cooper, J. *Phys. Rev. A* **1983**, *28*, 3349.
(45) Agarwal, G. S.; Haan, S. L.; Cooper, J. *Phys. Rev. A* **1984**, *29*, 2552; **1984**, *29*, 2565.
(46) Bialynicka-Birula, Z. *Phys. Rev. A* **1983**, *28*, 836.
(47) Bialynicka-Birula, Z. *J. Phys. B* **1983**, *16*, 4351.
(48) Zakrzewski, Z.; Rzażewski, K.; Lewenstein, M. *J. Phys. B* **1984**, *17*, 729.
(49) Kumelkov, S. E.; Perel', V. I. *Zh. Eksp. Teor. Fiz.* **1981**, *81*, 1693; *Sov. Phys. JETP (Engl. Transl.)* **1981**, *54*, 899.
(50) See, for example: Domcke, W. *J. Phys. B* **1981**, *14*, 4889.
(51) Brenig, W. *Z. Phys. B.: Condens. Matter Quanta* **1976**, *23*, 361.
(52) Brenig, W. *J. Phys. Soc. Jpn.* **1982**, *51*, 1914.
(53) Tsukada, M. *J. Phys. Soc. Jpn.* **1982**, *51*, 2927.